Sixth International Symposium on Turbulence and Shear Flow Phenomena
Seoul, Korea, 22-24 June 2009

TURBULENCE STRUCTURE FOR TWO- AND THREE-DIMENSIONAL ROUGHNESS

Karen A. Flack[1], Ralph J. Volino[1], Michael P. Schultz[2]
Department of Mechanical Engineering[1]
Department of Naval Architecture and Ocean Engineering[2]
United States Naval Academy
Annapolis, Maryland 21402 USA
flack@usna.edu, volino@usna.edu, mschultz@usna.edu

ABSTRACT

Turbulence measurements for a zero pressure gradient boundary layer over a two-dimensional roughness are presented and compared to previous results for a smooth wall and a three-dimensional roughness. The present experiments were made on transverse square bars in the fully-rough flow regime. The turbulence structure was documented through the fluctuating velocity components and two-point correlations of the fluctuating velocities. The 2-D bars lead to significant changes in the turbulence in the outer flow. Reynolds stresses, particularly $\overline{v'^2}^+$ and $-\overline{u'v'}^+$, increase, although the mean flow is not as significantly affected. Large scale turbulent motions originating at the wall lead to increased spatial scales in the outer flow. The dominant feature of the outer flow, however, remains hairpin vortex packets which have similar inclination angles for all wall conditions. The differences between boundary layers over 2-D and 3-D roughness are attributable to the scales of the motion induced by each type of roughness. Three-dimensional roughness produces turbulence scales of the order of the roughness height, k, while the motions generated by 2-D roughness may be much larger due to the width of the roughness elements.

INTRODUCTION

The importance of surface roughness is well known for wall-bounded flows. Roughness typically increases drag in turbulent boundary layers due to pressure forces on the roughness elements. While the flow structure near the roughness elements must be affected, Jiménez (2004) notes that as long as the roughness height, k, is not too large relative to the boundary layer thickness, δ, most of the evidence in the literature shows outer layer similarity between rough- and smooth-wall boundary layers. Roughness will alter the wall shear and the growth of the boundary layer, but when the outer flow is normalized using the friction velocity, u_τ, and δ, similarity is observed. This similarity was said to hold as long as k/δ <1/50. This is consistent with Townsend's (1976) Reynolds number similarity hypothesis. Schultz & Flack (2007) critically tested this hypothesis for the conditions proposed by Townsend ($k<<\delta$ and high Reynolds numbers), experimentally studying the boundary layer over a sanded surface. They considered cases ranging from the hydrodynamically smooth to the fully rough regimes and found excellent agreement in the Reynolds stresses and velocity triple products outside the near-wall region. Other studies since the Jiménez (2004) review include Flack, Schultz & Shapiro (2005), Kunkel & Marusic (2006), and Wu & Christensen (2007). All found outer layer similarity for boundary layers over various rough surfaces. Large roughness elements have also been tested. Castro (2007) conducted experiments with very large thee-dimensional (3-D) roughness (mesh, staggered cubes, gravel chips) and found that mean flow similarity held for k/δ <1/10. Flack, Schultz & Connelly (2007) observed outer layer similarity in turbulence quantities. They conducted experiments with 3-D mesh and sandpaper surfaces with a large range of roughness heights. They observed that roughness effects were confined to a roughness sublayer within $5k$ or $3k_s$ of the surface, where k_s is the equivalent sandgrain height. No critical value of k/δ was observed for breakdown of similarity. Effects of roughness were seen farther from the wall as $5k$ or $3k_s$ became a larger faction of δ.

Similarity in turbulence structure was reported by Volino, Schultz & Flack (2007) who experimentally studied boundary layers over a smooth wall and a wall covered with 3-D mesh. The turbulence structure was quantified through turbulence spectra, the probability density function of the swirl strength, two-point spatial correlations of turbulence quantities and swirl, structure angles and length scales of correlations. The dominant structure in both the rough-wall and smooth-wall outer layer was the vortex packet. Wu & Christensen (2007) reported similarity in the outer layer turbulence structure for flows over smooth walls and walls with replicated turbine blade roughness. Flores & Jiménez (2006) conducted a DNS study of a symmetric channel flow with 3-D disturbances on both bounding walls. The effect of the disturbances was confined to a layer near the wall. The structure and dynamics of the turbulence in the outer flow was virtually unchanged by the nature of the wall.

The studies noted above all considered 3-D k-type roughness. The consensus of most studies is that outer layer similarity with smooth wall boundary layers holds for a large range of 3-D roughness types and sizes. Two-dimensional k-type roughness may, however, cause different behavior. Two-dimensional transverse rods were studied by Krogstad & Antonia (1999). They reported an increase in the Reynolds stresses in the outer layer in comparison to smooth-wall results. The Reynolds stress profile shapes were significantly altered over the 2-D rods. The streamwise rod spacing, p, in this case was four times

the rod diameter. Keirsbulck *et al.* (2002) reported results for boundary layer experiments with 2-D transverse bars and p/k=3.33. They found reasonable similarity with smooth-wall flows for the Reynolds stresses in the outer flow. Djenidi *et al.* (2008) conducted experiments with 2-D transverse square bars and p/k ranging from 8 to 16. They noted differences in the turbulence structure and larger Reynolds stresses in the outer layer than for smooth wall cases. Results varied with bar spacing, with the strongest effect at larger spacing. This variation may explain the lesser effect of roughness observed by Keirsbulck *et al.* (2002), who used a smaller spacing. Lee & Sung (2007) conducted a DNS for a turbulent boundary layer over a wall with 2-D disturbances. The disturbances modeled 2-D transverse square bars with p/k=8. Lee & Sung (2007) reported an increase of all the Reynolds normal stresses and the Reynolds shear stress across most of the boundary layer. Velocity triple products in the outer layer, particularly the vertical transport of the Reynolds shear stress, were also affected by the roughness.

The present study focuses on the general question of whether 2-D and 3-D roughness affect turbulent boundary layers differently. This question is addressed through documentation of turbulence statistics and spatial correlations in turbulent boundary layers over walls with 2-D and 3-D roughness.

EXPERIMENTAL PROCEDURES

The test wall was an acrylic plate machined with 2-D transverse square bars, as shown in Fig. 1. The bar height was k=1.7 mm and the bar spacing was p/k=8. This geometry is expected to behave as k-type roughness according to Perry, Schofield & Joubert (1969). The roughness geometry is identical to that used in the DNS boundary layer study of Lee & Sung (2007) and the channel flow study of Krogstad *et al.* (2005). Smooth and 3-D rough wall comparison cases were documented in Volino *et al.* (2007). An acrylic test plate was used for the smooth-wall case. A woven wire mesh was affixed to a similar plate for the 3-D rough-wall case. The mesh spacing was t=1.69 mm, and the mesh wire diameter was 0.26 mm, resulting in a peak to trough roughness height of k=0.52 mm. The height of the mesh roughness is smaller than the present bar height. Flack, *et al.* (2007) studied the flow over sandgrain and mesh roughness for a wide range of roughness sizes, and observed similarity with smooth wall results in all cases. Included were cases with the ratio of the roughness height to boundary layer thickness smaller than the mesh of Volino *et al.* (2007) and cases with this ratio larger than that of the bars in the present study. The difference in roughness height between the mesh and the bars is not, therefore, expected to affect the results.

Boundary layer velocity measurements were obtained with a TSI FSA3500 two-component laser Doppler Velocimeter (LDV). The LDV consists of a four beam fiber optic probe that collects data in backscatter mode. A 2.6:1 beam expander was located at the exit of the probe to reduce the size of the measurement volume. The resulting probe volume diameter was 45 μm with a probe volume length of 340 μm. The corresponding measurement volume diameter and length in viscous length scales were d^+ = 1.5 and l^+ = 11.6.

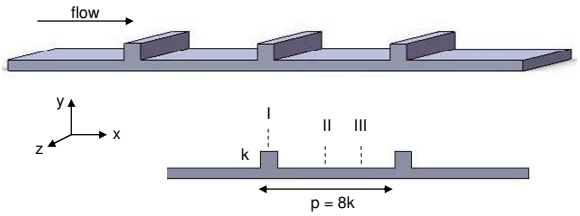

Figure 1. Schematic of 2-D bar roughness.

Measurements were made 1.0 m downstream of a 0.8 mm diameter wire trip, where the turbulent Reynolds number matched the value of the smooth wall comparison case. The LDV probe was traversed to approximately 40 locations within the boundary layer. A total of 50,000 random velocity samples were obtained at each location in the boundary layer. The data were collected in coincidence mode. The flow was seeded with 3 μm diameter alumina particles. Measurements were made at three streamwise stations over one roughness bar spacing as shown in Fig. 1. Station I was located at the center of a roughness element, station II was located 3k downstream of station I, and station III was located 5.75k downstream of station I. These are the same locations used by Lee & Sung (2007).

Flowfield measurements were acquired using particle image velocimetry (PIV). A streamwise-wall normal (xy) plane was acquired at the spanwise centerline of the test section. The flow was seeded with 3 μm diameter alumina particles. The light source was a Nd:YAG laser set for an 850 μs interval between pulses for each image pair. The field of view in the xy plane was 135 mm × 100 mm, extending from near the wall into the freestream. A CCD camera with a 1376×1024 pixel array was used. Image processing was done with TSI Insight 3G software. Velocity vectors were obtained using 16 pixel square windows with 50% overlap. For each measurement plane, 2000 image pairs were acquired for processing. Further experimental details, as well as the data processing techniques used to compute the mean velocity, turbulence statistics, wall shear and spatial correlations are described in detail in Schultz & Flack (2007) and Volino *et al.* (2007).

RESULTS

The boundary layer thickness, friction velocity and other quantities from the velocity profile of the present case and the comparison cases are presented in Table 1. The results presented were taken at station II (Fig. 1). No significant variation was observed in the results from the three stations except for a region within about 3k of the wall. For the rough-wall cases, the roughness Reynolds numbers based the equivalent sand roughness height, $k_s^+=k_s u_\tau/\nu$, are 112 (3-D) and 755 (2-D), indicating fully rough conditions. The ratio of roughness height to boundary layer thickness (k/δ) was 0.014 and 0.031 for the 3-D and 2-D cases, respectively. The Clauser chart method was used to evaluate u_τ, and the resulting values agreed with those from the total stress method to within 2%. Details of both methods are given in Flack *et al.* (2005).

Table 1. Boundary Layer Parameters

Wall	x [m]	U_e [m/s]	δ [mm]	u_τ [m/s]	Re_θ	Re_τ
Smooth	1.50	1.255	35.2	0.0465	6069	1772
3-D Mesh	1.08	1.247	36.8	0.0603	7663	2438
2-D Bars	1.00	0.50	54.6	0.0341	4260	1790

Mean Velocity and Turbulence Profiles

Mean velocity profiles for the cases in Table 1 are shown in Fig. 2 in both inner and defect coordinates. The inner normalized coordinates show a much larger shift for the 2-D roughness. No clear differences are visible in defect coordinates. Similarity in the mean profiles was also noted by Krogstad & Antonia (1999) for 2-D and 3-D roughness. These results indicate that the mean flow in the outer layer is fairly insensitive to surface conditions.

The Reynolds stresses for the 2-D and 3-D roughness cases in outer coordinates are compared to the smooth-wall results in Figs. 4-6. Also shown are the 2-D roughness results of Krogstad & Antonia (1999), who used rods spaced at p/k=4. The $\overline{u'^2}^+$ normal stress is shown in Fig. 3. The present 2-D roughness values in the outer layer are somewhat higher than in the comparison cases, but the differences are not large. The $\overline{v'^2}^+$ normal stress is shown in Fig. 4. The 2-D roughness results of the present study and Krogstad & Antonia (1999) agree, and are roughly 20% higher than in the 3-D rough- and smooth-wall cases. The difference extends well into the outer region to y/δ of about 0.7. Similar differences are present in the Reynolds shear stress, shown in Fig. 5. Differences in $\overline{v'^2}^+$ and $-\overline{u'v'}^+$ were

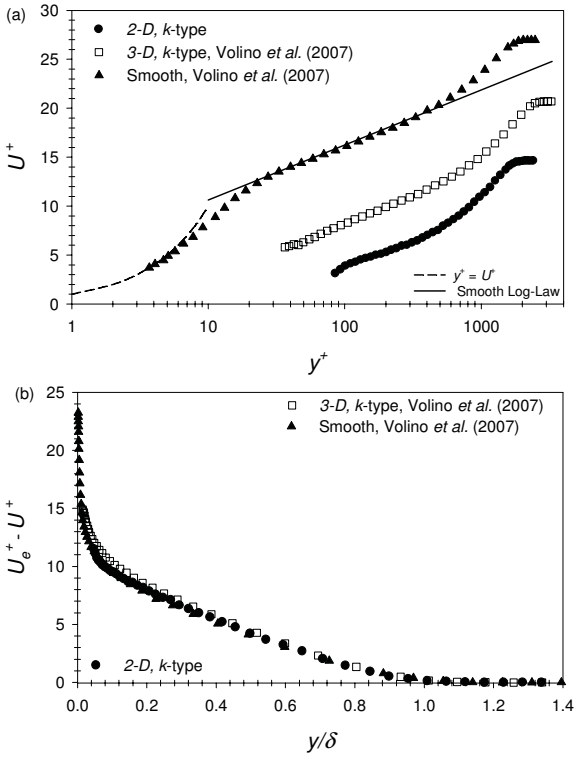

Figure 2. Mean velocity profiles in a) inner variables, b) velocity defect form.

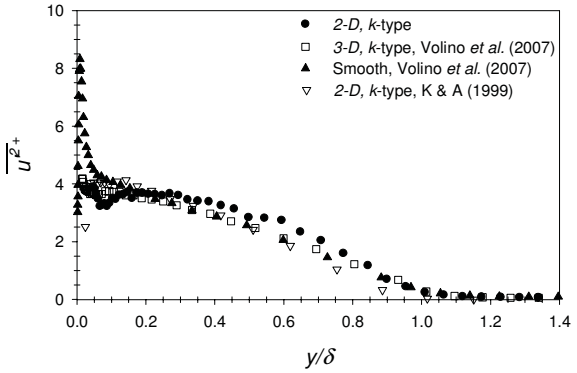

Figure 3. Streamwise Reynolds normal stress profiles.

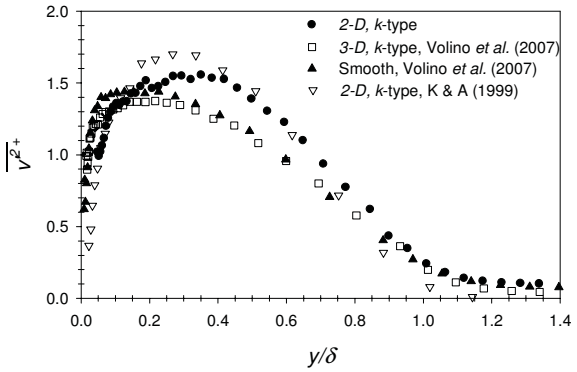

Figure 4. Wall-normal Reynolds normal stress profiles.

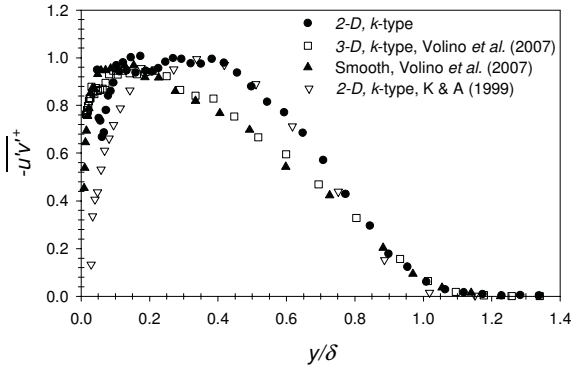

Figure 5. Reynolds shear stress profiles.

also noted in the outer layer by Lee and Sung (2007), however they also documented similar increases in $\overline{u'^2}^+$.

The present results along with the body of literature show that 2-D roughness affects the boundary layer differently than 3-D roughness. Outer layer similarity with the smooth-wall case is disrupted. The 2-D bars must affect the turbulence structure in the outer flow, which is considered next.

Velocity Fields, xy Plane

Typical instantaneous velocity vector fields in the streamwise-wall normal plane are shown in Fig. 6 for the 2-D and 3-D wall cases. A uniform convection velocity $0.7U_e$ subtracted from each field. The hairpin vortices in a packet become visible if their common convection velocity is subtracted from the instantaneous field. Hairpin packets typically appear as a line of vortices, inclined at about 10° to 15° to the wall. In the 3-D rough-wall case (Fig. 6a) a

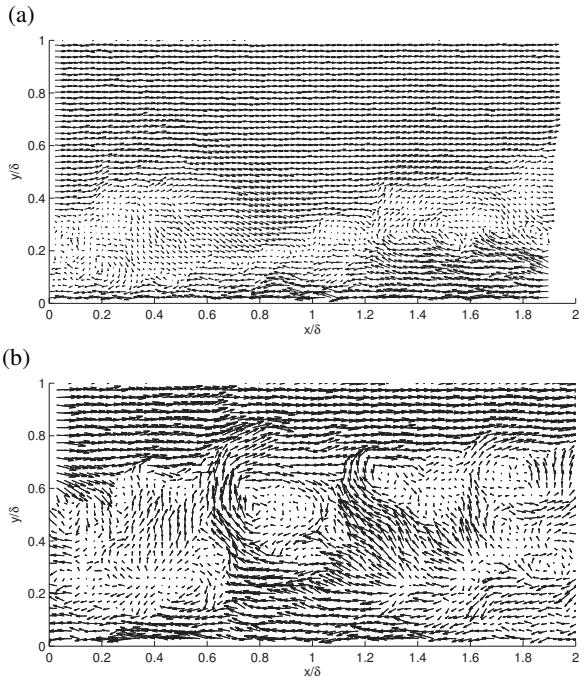

Figure 6. Typical instantaneous velocity field in *xy* plane.

field has been chosen which shows the end of a mature hairpin packet on the left (x/δ<0.6) with another hairpin packet extending nearly the entire width of the image (0<x/δ<1.9). Such packets did not appear in every instantaneous field, but they were very common for both the 3-D rough- and the smooth-wall cases, as shown in Volino *et al.* (2007). Similar packets were also observed in the 2-D rough-wall case, but they were also accompanied by larger scale events, as shown in Fig. 6b. Figure 6b shows large scale eruptions of fluid extending to the edge of the boundary layer. Events extending this far into the outer part of the boundary layer were very rare in the smooth- and 3-D rough-wall cases, but they were fairly common in the 2-D rough-wall case, appearing in roughly 10% of the instantaneous velocity fields.

The large scale events are believed to originate on the wall at the bars. In the various studies listed above with close-packed 3-D roughness, large contiguous open spaces between the roughness elements were not present, so recovery of the instantaneous velocity profile in the valleys between roughness elements seems unlikely. The flow would tend to move around and over the tops of the 3-D roughness elements, with low velocity or stagnant fluid near the base of the elements. In cases with sparse 3-D roughness (e.g. the coarsest sandgrain roughness cases of Flack *et al*., 2007), some separation would occur from individual elements, but much of the flow could remain attached to the surface as it moved around the sides of the elements. With the 2-D bars, flow around the sides of the bars is impossible since they block the entire span. Also, one might imagine that after the boundary layer is disrupted by a bar, it has a chance to at least approach reattachment between bars. In instances where the reattachment is somewhat complete, fluid with nonzero velocity could impact the full face of the subsequent bar instead of just the top of the element. The bar would then act as a trip and produce a larger disturbance than a field of 3-D elements of the same height.

The average extent and shape of the hairpin packets can be quantified through two-point correlations of the fluctuating velocity. Figures 7a-c show contours of the two-point correlations of the streamwise fluctuating velocity, R_{uu}, with the correlation centered at y_{ref}/δ=0.4. The 3-D rough- and smooth-wall results appear similar. The correlation for the 2-D rough case has the same shape as in the other cases, but has a noticeably larger extent in both the streamwise and wall normal directions.

The angle of inclination of R_{uu} is related to the average inclination of the hairpin packets. It was determined, as in Volino *et al.* (2007), using a least squares method to fit a line through the points farthest from the self correlation peak on each of the five R_{uu} contour levels 0.5, 0.6, 0.7, 0.8 and 0.9 both upstream and downstream of the self correlation peak. For the present cases, the inclination angle remains nearly constant for reference points between y/δ=0.2 and 0.5. For y/δ <0.2 the angle drops somewhat as the contours begin to merge with the wall. For y/δ >0.5 the angle decreases toward zero, as these points tend to be above the hairpin packets which produce the inclination. For 0.2<y/δ <0.5, the angles are 10.2°± 2.7°, 11.3°± 2.2° and 10.6°±1.2° for the smooth, 3-D rough and 2-D rough walls respectively. The range in each case indicates the span about the average observed between y/δ =0.2 and 0.5. The difference between the cases is comparable to the scatter in the data and the range reported in the literature for smooth-wall boundary layers (e.g. Adrian, Meinhart & Tomkins, 2000). Therefore the large scale events noted in Fig. 7 do not significantly affect the structure angle.

The streamwise and wall normal extent of R_{uu} are shown in Figs. 7d and 7e as a function of the reference point. The distance, Lx_{uu}, is defined as in Christensen & Wu (2005) as twice the distance from the self correlation peak to the most downstream location on the R_{uu}=0.5 contour. The 3-D rough- and smooth-wall results agree very well, but the 2-D rough-wall value averages 42% larger. The wall normal extent of the R_{uu} correlation, Ly_{uu}, is determined based on the wall normal distance between the points closest and farthest from the wall on a particular contour. Figure 8e shows Ly_{uu}/δ as a function of y/δ using the R_{uu}=0.5 contour. Due to the contours merging with the wall, Ly_{uu} drops toward zero for y/δ <0.2. As with Lx_{uu}, the 3-D rough- and smooth-wall results agree well. The Ly_{uu} value averages 39% higher for the 2-D rough wall case.

Figure 8 shows R_{vv} contours centered at y/δ=0.4 along with Lx_{vv} and Ly_{vv} as functions of y/δ. The length Lx_{vv} is determined based on the streamwise distance between the most upstream and downstream points on the R_{vv}=0.5 contour. The length Ly_{vv} is defined as above for the R_{uu} results. The streamwise extent of R_{vv} is considerably less than that of R_{uu}, since R_{uu} is tied to the common convection velocity of each hairpin packet. The ratio Lx_{vv}/Ly_{vv} is about 0.8 for all walls. Both the streamwise and wall normal length scales are essentially equal for the smooth and 3-D rough-walls, and average 35 and 40% larger on the 2-D rough wall for Lx_{vv} and Ly_{vv} respectively.

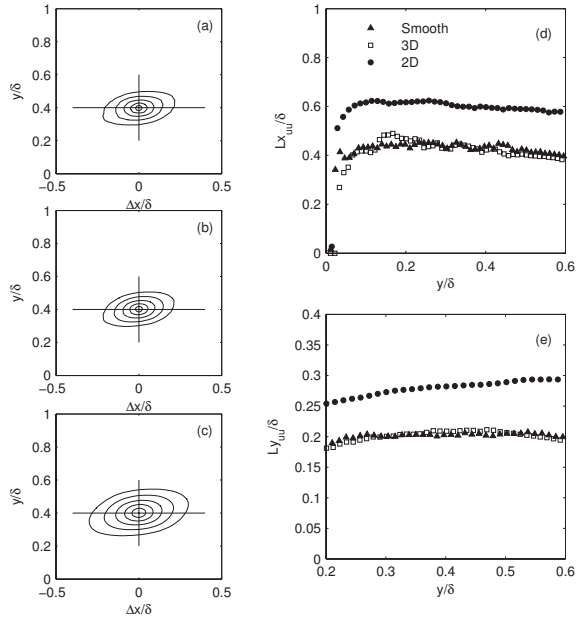

Figure 7. Contours of R_{uu} centered at y/δ=0.4, outermost contour R_{uu}=0.5, contour spacing 0.1, a) smooth wall, b) 3-D rough wall, c) 2-D rough wall; d) Streamwise extent of R_{uu}=0.5 contour as function of y/δ, e) Wall normal extent of R_{uu}=0.5 contour as function of y/δ.

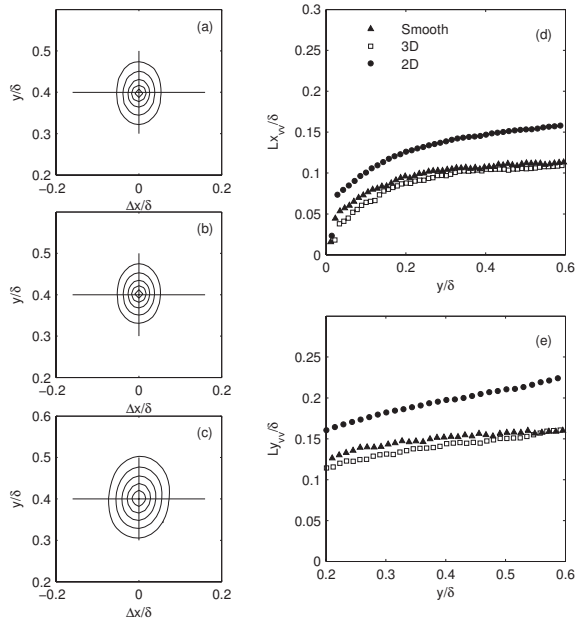

Figure 8. Contours of R_{vv} centered at y/δ =0.4, outermost contour R_{vv}=0.5, contour spacing 0.1, a) smooth wall, b) 3-D rough wall, c) 2-D rough wall; d) Streamwise extent of R_{vv}=0.5 contour as function of y/δ, e) Wall normal extent of R_{uu}=0.5 contour as function of y/δ.

Contours of the cross-correlation R_{uv} centered at y/δ=0.4 are shown in Fig. 9 along with Lx_{uv} and Ly_{uv} as functions of y/δ. The lengths are computed as for R_{vv}, but are based on the -0.15 contour. As with R_{uu} and R_{vv}, the smooth- and 3-D rough-wall results are essentially equal. For the 2-D rough wall, Lx_{uv} averages 36% larger and Ly_{uv} averages 45% larger than in the comparison cases.

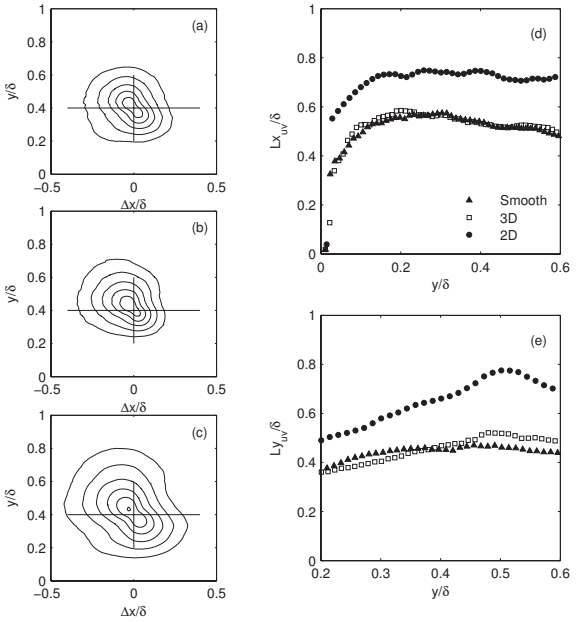

Figure 9. Contours of R_{uv} centered at y/δ=0.4, outermost contour R_{uv}=-0.15, contour spacing -0.05, a) smooth wall, b) 3-D rough wall, c) 2-D rough wall; d) Streamwise extent of R_{uv}=-0.15 contour as function of y/δ, e) Wall normal extent of R_{uv}=-0.15 contour as function of y/δ.

In summary, the shapes of the two point correlations are similar for all three walls, but the spatial extent of the correlations is about 40% larger for the 2-D rough-wall case. This is consistent with the presence of the large scale motions noted in Fig. 6b for the 2-D rough-wall case. The above results also show a clear difference between flows over 3-D and 2-D roughness due to the large scale ejections into the outer boundary layer caused by 2-D roughness. This has been quantified through the large k_s/k ratio associated with the 2-D roughness. As shown through flow visualization by Furuya *et al.* (1976), the flow between 2-D bars is able to recover and approach reattachment, resulting in a large event when it impacts the next bar. Furuya *et al.* (1976) showed that if the bars are close together, the recovery is less complete, and the disturbances created are smaller. There is an optimal p/k for creating large disturbances as frequently as possible, and as noted by Krogstad *et al.* (2005), it is near the p/k=8 used in the present study. Since the large structures in the 2-D case are believed to originate at the bars, they indicate a direct connection of the outer flow to the wall. They would be attached eddies in the terminology of Perry & Chong (1982). In the smooth-wall and 3-D rough-wall cases, the outer part of the boundary layer contains only detached eddies (Perry & Marusic, 1995), which have separated from the wall.

CONCLUSIONS

An experimental study has been carried out in a turbulent boundary layer over two-dimensional roughness. Comparison with previous results indicates the present roughness leads to significant changes in the turbulence in the outer flow. An increase in the Reynolds stresses, particularly $\overline{v'^2}^+$ and $-\overline{u'v'}^+$, was observed. The mean flow

was not as significantly affected. These results are consistent with the 2-D roughness results of Krogstad & Antonia (1999). The difference in the Reynolds stresses was due to large scale turbulent motions emanating from the wall. These motions are associated with attached eddies, as described by Perry & Chong (1982). The large scale attached eddies lead to an increasing spatial scale in the outer flow. The turbulence structure, however, was qualitatively similar to that observed over smooth and 3-D rough walls. The dominant feature of the outer flow was hairpin vortex packets having similar inclination angles in all cases. The differences observed between boundary layers over 2-D and 3-D roughness are attributable to the scales of the motion induced in each case. The largest scale motions generated by 3-D roughness are of the order of the roughness height, k, while the motions generated by 2-D roughness may be much larger than k due to the width of the roughness elements.

REFERENCES

Adrian, R. J., Meinhart, C. D. & Tomkins, C. D., 2000, "Vortex organization in the outer region of the turbulent boundary layer," *J. Fluid Mech.,* Vol. 422, pp. 1-54.

Castro, I. P., 2007, "Rough-wall boundary layers: mean flow universality," *J. Fluid Mech.,* Vol. 585, pp. 469-485.

Christensen, K. T. and Wu, Y., 2005, "Characteristics of vortex organization in the outer layer of wall turbulence," *Proceedings of Fourth International Symposium on Turbulence and Shear Flow Phenomena*, Williamsburg, Virginia, Vol. 3, pp. 1025-1030.

Djenidi, L., Antonia, R. A., Amielh, M. and Anselmet, F., 2008, "A turbulent boundary layer over a two-dimensional rough wall," *Exps. Fluids*, Vol. 44, pp. 37-47.

Flack, K. A., Schultz, M. P., and Connelly, J. S., 2007, "Examination of a critical roughness height for boundary layer similarity," *Phys. Fluids*, Vol. 19, Article #095104.

Flack, K. A., Schultz, M. P. and Shapiro, T. A., 2005, "Experimental support for Townsend's Reynolds number similarity hypothesis on rough walls," *Phys. Fluids*, Vol. 17, Article #035102.

Flores, O. and Jiménez, J., 2006, "Effect of wall-boundary disturbances on turbulent channel flows," *J. Fluid Mech.,* Vol. 566, pp. 357-376.

Furuya, Y., Miyata, M. and Fujita, H., 1976, "Turbulent boundary layer and flow resistance on plates roughened by wires," *J. Fluids Engineering*, Vol. 98, pp. 635-644.

Jiménez, J., 2004, "Turbulent flows over rough walls," *Annu. Rev. Fluid Mech*, Vol. 36, pp. 173-196.

Keirsbulck, L., Labraga, L., Mazouz, A. and Tournier, C., 2002, "Surface roughness effects on turbulent boundary layer structures," *J. Fluids Engineering*, Vol. 124, pp. 127-135.

Krogstad, P.-Å. and Antonia, R. A., 1999, "Surface roughness effects in turbulent boundary layers," *Exps. Fluids*, Vol. 27, pp. 450-460.

Krogstad, P.-Å., Andersson, H. I., Bakken, O. M. and Ashrafian, A., 2005, "An experimental and numerical study of channel flow with rough walls," *J. Fluid Mech.*, Vol. 530, pp. 327-352.

Kunkel, G. J. and Marusic, I., 2006, "Study of the near-wall-turbulent region of the high-Reynolds-number boundary layer using an atmospheric flow," *J. Fluid Mech.*, Vol. 548, pp. 375-402.

Lee, S. H. and Sung, H. J., 2007, "Direct numerical simulation of the turbulent boundary layer over a rod-roughened wall," *J. Fluid Mech.*, Vol. 84, pp. 125-146.

Perry, A. E. and Chong, M. S., 1982, "On the mechanism of wall turbulence," *J. Fluid Mech.,* Vol. 119, pp. 173-217.

Perry, A. E. and Marusic, I., 1995, "A wall-wake model for the turbulence structure of boundary layers. Part 1. Extension of the attached eddy hypothesis," *J. Fluid Mech.*, Vol. 298, pp. 361-388.

Perry, A. E., Schofield, W. H. and Joubert, P., 1969, "Rough wall turbulent boundary layer," *J. Fluid Mech.*, Vol. 165, pp. 163-199.

Schultz, M. P. and Flack, K. A., 2007, "The rough-wall turbulent boundary layer from the hydraulically smooth to the fully rough regime," *J. Fluid Mech.*, Vol. 580, pp. 381-405.

Townsend, A. A., 1976, *The Structure of Turbulent Shear Flow*. 2nd Edition, Cambridge University Press.

Volino, R. J., Schultz, M. P. & Flack, K. A., 2007, "Turbulence structure in rough- and smooth-wall boundary layers," *J. Fluid Mech.*, Vol. 592, pp. 263-293.

Wu, Y. and Christensen, K. T., 2007, "Outer-layer similarity in the presence of a practical rough-wall topography," *Phys. Fluids*, Vol. 19, Article #085108.